HHS Public Access

Author manuscript

Oncogene. Author manuscript; available in PMC 2017 January 27.

Published in final edited form as:

Oncogene. 2017 January 26; 36(4): 491–500. doi:10.1038/onc.2016.218.

MUC13 Interaction with Receptor Tyrosine Kinase HER2 Drives Pancreatic Ductal Adenocarcinoma Progression

Sheema Khan[1], **Mohammed Sikander**[1], **Mara C. Ebeling**[2], **Aditya Ganju**[1], **Sonam Kumari**[1], **Murali M. Yallapu**[1], **Bilal Bin Hafeez**[1], **Tomoko Ise**[3], **Satoshi Nagata**[3], **Nadeem Zafar**[4], **Stephen W. Behrman**[5], **Jim Y. Wan**[6], **Hemendra M. Ghimire**[7], **Peeyush Sahay**[7], **Prabhakar Pradhan**[7], **Subhash C. Chauhan**[1,*], and **Meena Jaggi**[1,*]

[1]Department of Pharmaceutical Sciences and Center for Cancer Research, University of Tennessee Health Science Center, Memphis, Tennessee, USA

[2]Cancer Biology Research Center, Sanford Research, Sioux Falls, South Dakota, USA

[3]Center for Drug Design Research, National Institutes of Biomedical Innovation, Health and Nutrition (NIBIOHN), Ibaraki-City, Osaka, Japan

[4]Department of Pathology, University of Tennessee Health Science Center, Memphis, Tennessee, USA

[5]Department of Surgery, University of Tennessee Health Science Center, Memphis, Tennessee, USA

[6]Department of Biostatistics & Epidemiology, University of Tennessee Health Science Center, Memphis, Tennessee, USA

[7]Department of Physics, University of Memphis, Memphis, Tennessee, USA

Abstract

Although MUC13, a transmembrane mucin, is aberrantly expressed in pancreatic ductal adenocarcinoma (PDAC) and generally correlates with increased expression of HER2, the underlying mechanism remains poorly understood. Herein, we found that MUC13 co-localizes and interacts with HER2 in PDAC cells (reciprocal co-immunoprecipitation, immunofluorescence, proximity ligation, co-capping assays) and tissues (immunohistofluorescence). The results from this study demonstrate that MUC13 functionally interacts and activates HER2 at p1248 in PDAC cells, leading to stimulation of HER2 signaling cascade including, ERK1/2, FAK, AKT and PAK1 as well as regulation of the growth, cytoskeleton remodeling and motility and invasion of PDAC cells - all collectively contributing to PDAC progression. Interestingly, all of these phenotypic effects of MUC13-HER2 co-localization could be effectively compromised by depleting MUC13

*Corresponding Authors: Subhash C. Chauhan, Ph.D., Professor, Department of Pharmaceutical Sciences, University of Tennessee Health Science Center, 19 South Manassas, Cancer Research Building, Memphis, TN, 38163. Phone: (901) 448-2175. Fax: (901) 448-1051. schauha1@uthsc.edu. Meena Jaggi, PhD., Associate Professor, Department of Pharmaceutical Sciences, University of Tennessee Health Science Center, 19 South Manassas, Cancer Research Building, Memphis, TN, 38163. Phone: (901)-448-6848. Fax: (901)-448-1051. mjaggi@uthsc.edu.

Supplementary Information accompanies the paper on the Oncogene website (http://www.nature.com/onc).

and mediated by the first and second EGF-like domains of MUC13. Further, MUC13-HER2 co-localization also holds true in PDAC tissues with a strong functional correlation with events contributing to increased degree of disorder and cancer aggressiveness. In brief, findings presented here provide compelling evidence of a functional ramification of MUC13-HER2: this interaction could be potentially exploited for targeted therapeutics in a subset of patients harboring an aggressive form of PDAC.

Keywords

Cancer; Mucin; MUC13; HER2; Interaction; Morphological distortion

Introduction

Protein-protein interaction networks have important roles in cellular functions and biological processes [1]. MUC13, a transmembrane mucin, is known to be aberrantly expressed in pancreatic ductal adenocarcinoma (PDAC) [2]. MUC13 has a large tandem repeat domain, 3 epidermal growth factor (EGF)-like domains, a sea urchin sperm protein enterokinase arginine (SEA) domain and a trans-membrane domain containing a cytoplasmic domain [3]. The interaction of MUC13 with other proteins is under study and demands further investigation to understand their transition to disease promotion. Our previous studies demonstrate that the over-expression of MUC13 leads to up-regulation and tyrosine phosphorylation of HER2 in PDAC cells [2]. HER2 belongs to the human epidermal growth factor receptor (EGFR/ErbB) family of receptor tyrosine kinases that have been widely implicated in human cancers [4] and cancer pathogenesis [5]. Although it is understood that receptor activation requires interactions between their specific ligands, so far, no soluble ligand has been identified for HER2. However, reports suggest that activation of ErbB receptors can be potentiated by proteins such as mucins, like MUC1 and MUC4 [6]. The present study involves the identification of novel interactions of MUC13 with HER2 in PDAC. MUC13 consists of three EGF-like domains that may serve as a ligand for EGF receptors, such as HER2, and modulate EGFR signaling pathways. This investigation, for the first time, elucidates that MUC13 may act as a ligand to HER2 through which it drives important signaling pathways in PDAC.

Results

MUC13 Interacts with HER2 Oncoprotein in PDAC Cells

Previous studies showed that MUC13 expression increases expression of HER2 in multiple cell types and MUC13 knockdown was accompanied by downregulation of HER2 expression [2]. Therefore, in this study, we investigated the direct association of MUC13 and HER2 in PDAC cells. Co-localization experiments applying antibody-induced double immunofluorescence staining techniques indicated that MUC13 and HER2 are interacting partners in PDAC cells. We observed a strong co-localization (Fig. 1A, yellow) of MUC13 (Fig. 1A, green) and HER2 (Fig. 1A, red) in both membrane and cytoplasmic regions of cells. The co-localization was observed to be predominant at the membrane of HPAF-II cells (Fig. 1A). Additionally, reciprocal immunoprecipitation analyses showed that HER2 is

pulled down in MUC13 immunoprecipitates and vice versa (Fig. 1B and S1). The IgG (Fig. 1B) served as an internal control and MUC13 null Panc-1 cells as negative controls (Fig. S2A).

Proximity ligation assay (PLA) is a recently developed technique to determine protein-protein interaction in close proximity (30–40 nm). Thus, to validate the interaction between MUC13 and HER2 and to retrieve information about the subcellular location of the interaction, we performed PLA using antibodies targeting MUC13 and HER2 or β-catenin as a negative control. PLA enables direct observation of individual endogenous protein complexes and detects the interactions among two proteins *in situ*. Our investigations revealed that in PDAC cells, HER2 and MUC13 are expressed in close proximity of each other as observed by the multiple red spots in the membrane (Fig. 1C). The β-catenin with E-cadherin served as an experimental positive control as they are reported to physically interact in cells[7].

We further confirmed our observations through MUC13-HER2 co-capping experiments in HPAF-II and AsPC-1 cells. HPAF-II and AsPC-1 cells showed progressively increasing distribution of membrane staining into caps (75%) (Fig. 2A). Panc-1 cells that are MUC13 null served as an internal negative control (Fig. 2A). As an experimental negative control, a similar capping experiment was performed with α-tubulin in HPAF-II cells (Fig. 2B) which did not cocluster with MUC13. This clearly suggests that MUC13 and HER2 coexist in PDAC cells and their association may be of high biological significance in PDAC cells.

MUC13 Regulates HER2 Associated Downstream Signaling Pathways

Our previous studies show that MiaPaca cells stably expressing MUC13 have increased HER2 expression whereas MUC13 knockdown PDAC cells show decreased levels of HER2 expression [2]. We further validated this finding by examining it in another MUC13-null cell line, Panc-1, that was stably transfected with MUC13 to confirm that this was not a cell specific response in stable cultures. Panc-1-M13 was selected for further analysis due to its high MUC13 expression as determined by Western blotting (Fig. 3A) and RT-PCR as previously described [2]. Interestingly, we observed increased levels of HER2 expression in MUC13 expressing Panc-1-M13 cells and reduced HER2 expression in shMUC13A cells (Fig. S2B). This confirmed that MUC13 expression could indeed alter HER2 expression.

Next, we sought to determine whether the interaction of MUC13 and HER2 potentiated HER2 mediated downstream signaling. HER2 is known to regulate cell proliferation, migration and invasion by activating downstream MAPK and PI3K/AKT pathways [8]. The presence of three EGF like domains in MUC13 suggests that MUC13 may contribute to pancreatic tumorigenesis through its interaction with EGFRs like HER2. We speculated that EGF like domains of MUC13 may serve as a binding site for HER2 to modulate its stabilization, recycling, and activation. These events could modulate the EGF receptor cascade and its downstream signaling that leads to excessive proliferation, invasion and metastasis [8]. We investigated this possibility by examining the level of HER2 and its major autophosphorylated form (pY1248-HER2) in MUC13 expressing Panc-1-M13. A marked increase in the level of both HER2 and its phosphorylated form was observed in MUC13 expressing Panc-1 cells compared to MUC13 null Panc-1 cells (Fig. 3A). Consistent with

our previous observations, further investigations revealed an activation of downstream targets of HER2, such as PAK1, ERK (p42/44 MAPK) and p-AKT that are key effectors of the PI3K/AKT and MAPK signal transduction pathways in tumor progression (Fig. 3A and 3B) [8].

Additionally, MUC13 expressing Panc-1-M13 cells showed significantly increased activation of Focal adhesion kinase (FAK), another downstream effector of HER2 [5], as indicated by increased expression of $pFAK^{Y925}$ (Fig. 3A). The phosphorylation of FAK at tyrosine 925 is required for its activation and subsequent role in integrating signals from integrins and receptor tyrosine kinases in processes such as cell survival, proliferation migration and invasion [9, 10]. Additionally, functional analysis reveals that the ectopic expression of MUC13 in MUC13 null Panc-1 cells (Panc-1-M13) resulted in the increase of their clonogenicity and migratory potential (Fig. S2C and S2D). All these observations suggest that MUC13 activates HER2 signaling cascade that leads to excessive proliferation, invasion and metastasis.

MUC13 Regulates HER2 Mediated Actin Reorganization

Oncogenic transformation initiates the motility function in many tissues leading to reorganization of their cytoskeleton and cell shape [11]. Because the activation of PAK-1 has been shown to result in phenotypic changes and actin remodeling through its interaction with HER2 [12, 13], we explored the potential involvement of MUC13 in F-actin remodeling. Our immunoblotting (Fig. 3B) and immunofluorescence (Fig. S3A) experiments reveal that MUC13 expressing cells have significantly increased expression of p-PAK1 and PAK-1, which are correlated with an increase in HER2 expression. We compared the alterations of F-actin and its organization in exogenous MUC13 expressing MiaPaca cells and MUC13 knockdown HPAF-II (shMUC13A) cells. We observed significantly increased levels of F-actin expression on leading edges in MUC13 expressing MiaPaca-M13B (Fig. S3A) cells and reduced F-actin expression in MUC13 knockdown HPAF-II (shMUC13A) cells (Fig. S3B). The increased expression of HER2 and its interaction with PAK-1 are prerequisites for the reorganization of actin cytoskeleton [12, 13]. Therefore, the increased expression of PAK-1 and F-actin in MUC13 expressing cells suggests the role of HER2/PAK-1 dependent reorganization of actin cytoskeleton in MUC13-mediated enhanced migration/invasion of PDAC cells.

Next, we tested the possibility that MUC13, in addition to actin reorganization, may also influence the organization of integrins and promote assembly of adhesion complexes to enhance growth factor signaling. Although not remarkable, our confocal microscopy images revealed enhanced integrin-α5 and vinculin clustering at the focal adhesions of Panc-1-M13 cells as compared to Panc-1-V cells (Fig. 3C). Therefore, we examined whether MUC13 facilitates integrin mediated adhesion to various ECM components and performed cell adhesion assays. The MUC13 expressing Panc-1-M13 cells showed significantly lower ($P < 0.05$) adherence to collagen I and fibronectin coated wells compared with the MUC13 null Panc-1-V cells (Fig. 3D). These results suggest that the overexpression of MUC13 in pancreatic tumors reduces the ability of tumor cells to interact with ECM proteins. Next, we investigated the possible relationship between decreased adhesiveness and integrin

expression in MUC13 expressing versus MUC13 null cells that were seeded on integrin-coated (α4, α5) plates and allowed to adhere for 1.5 h. A significantly reduced adhesion ($P < 0.05$) of the Panc-1-M13 cells to the integrin-coated plates was observed compared with the Panc-1-V cells (Fig. 3E). The adhesion capability of Panc-1-M13 cells was found to be restored after capping the cells with MUC13 antibody before allowing to adhere on the integrin coated plates. This enabled the clustering/capping of the MUC13 molecules at the cell surface as one or more caps (Fig. 3F) and accompanied adhesion of Panc-1-M13 cells but not Panc-1-V to integrin coated plates. Since there was no change observed in the expression of integrin α5 by immunoblotting (Fig. 3G), the results suggest that MUC13, being a bulky glycoprotein, impedes integrin binding to its ligands by causing steric hindrance at the cell surface. MUC13 expression in PDAC cells has no influence on altering the integrin state to mediate adherence and activation of growth signaling mechanisms. However, MUC13 may influence the spatial distribution of integrins on focal adhesions.

MUC13 EGF-Like Domains Serve as Potential Binding Site for EGFRs

MUC13 consists of three EGF-like domains that can interact with EGFRs like HER2 and may contribute to tumorigenic signaling in PDAC [14, 15]. Therefore, we sought to investigate whether EGF-like domains interact with and activate the HER2. It is probable that these EGF-like domains might direct heterodimerization with ErbB receptors and mediate EGFR signaling. Thus, we generated three different deletion mutants of MUC13 with deletion mutations at EGF domains (Fig. 4A). We determined the tumorigenic characteristics associated with each domain of MUC13 by transient transfection of deletion mutant constructs in MUC13 null Panc-1 cells (Fig. 4B). We investigated the effect of EGF-like domain deletion mutants on the proliferation and invasion of the cells. MUC13 ΔEGF 2/3 and ΔEGF 1/3 exhibited increased proliferation and invasion of Panc-1 cells that was almost equal to Full length MUC13 (FL-MUC13), while MUC13 ΔEGF 1/2 failed to show any changes in cell proliferation and invasion and was comparable to EGFP vector control (Fig. 4C and D). In order to investigate the EGF-like domain of MUC13 that directly interacts with HER2, we performed reciprocal immunoprecipitation. The results clearly suggested interaction of HER2 with MUC13 ΔEGF 2/3 and ΔEGF 1/3 as HER2 was immunoprecipitated with both the MUC13 mutants but not with MUC13 ΔEGF 1/2 (Fig. 4E and F). This interaction was observed to increase the phosphorylation and total levels of HER2, FAK1, ERK and PAK1 (Fig. 4G), suggesting that MUC13-HER2 interaction regulates the stabilization and activation of HER2 and its downstream molecular events. Thus, these results further confirm that out of the three EGF-like domains that are present in MUC13, EGF-like domains (EGF1 and 2) are responsible in MUC13-HER2 interaction and the subsequent increased proliferation or invasion of cells as a result of HER2 activation. Thus, EGF-like domains of MUC13 may serve as potential binding sites for EGFRs like HER2.

HER2 activation is prerequisite to MUC13 induced cellular transformation

In order to evaluate the role of HER2 in MUC13 induced transformation of a cell phenotype, we performed HER2 knockdown in ectopically (Panc-1-M13) and endogenously (HPAF-II) MUC13 expressing cells (Fig. 5A and S4A). HER2 knockdown in Panc-1-M13 cells inhibited MUC13 induced phosphorylation of main downstream targets of MUC13, namely

ERK1/2, AKT, PAK1 and FAK (Fig. 5B and 5C). Additionally, the HER2 silencing was observed to abrogate the invasion and migration ability of both Panc-1-M13 (Fig. 5D and E) and HPAF-II (Fig. S4B and C) cells. These results clearly suggest the involvement of HER2 in MUC13 mediated tumorigenic characteristics in PDAC cells.

MUC13 co-localizes with HER2 in Human PDAC Tissue Samples

We also examined the normal human pancreatic, adjacent normal and cancer tissues for MUC13 and HER2 expression and their co-localization using immunohistofluorescence technique (Fig. 6A, B and 7A). Our observations clearly demonstrate the co-localization of MUC13 and HER2 as depicted by merging (yellow) of confocal microscopic images of MUC13 (red) and HER2 (green) (Fig. 6A and 7A). 83.9% of cancer samples were stained positive for MUC13, while 57.2% for HER2. We also observed MUC13 and HER2 staining in adjacent normal samples (51.2 and 17.9 %, respectively) but the intensity and the percentage of staining in each tissue sample varied considerably and were significantly less as compared to cancer samples. MUC13 and HER2 co-localization was observed to be significantly higher (38.1%; Chi-square p=0.0010) in cancer samples compared to the adjacent normal samples (10.2%), suggesting clinical relevance of this interaction (Fig. 6A, Inset 1 and 2 and 7A). The normal pancreatic samples did not show any MUC13 and HER2 co-localization. Interestingly, differential staining patterns of MUC13 and HER2 were observed in some cancer tissue samples and besides being strongly co-positive for both proteins, did not show their co-localization (Fig. 6B).

MUC13 and HER2 co-localization is Associated with Nanoscale Morphological Distortion in Nuclear Chromatin which Accounts for Increased Cancer Aggressiveness

During carcinogenesis, the chromatin organization in a cell gets rearranged and causes morphological distortion in the nucleus relative to its normal/control state. It has been shown that there is a strong correlation between the strength of the local morphological distortion (L_{md}) in nuclear chromatin structure and the cancer stage, both increase with the progression of carcinogenesis [16]. Therefore, quantification of the strength of the morphological distortion provides the stage or degree of aggressiveness of the cancer in a biological cell. The inhomogeneity nature of the biological cells makes the quantification of distortion fairly complicated. Therefore, an effective average distortion strength is calculated solving the properties of the normal modes of the light wave within the normal and cancerous cells. Herein, to determine the clinical significance of MUC13 and HER2 co-localization in carcinogenesis, we studied pancreatic ductal adenocarcinoma samples from different patient cases and determined the correlation of the degree of distortion with respect to the presence or absence of co-localization in different areas within the samples and/or individual samples. For this, mass arrays and then dielectric arrays were created from the confocal imaging of the cells, then the normal modes of light waves were obtained. This was followed by the quantification of the amount of the morphological distortion, L_{md}, by taking the average of the square of the intensity of the normal modes, using a very similar methodology described elsewhere[17–19].

The average L_{md} at specific length scale increases with the increase in the degree of disorder. Proportionality relation between morphological distortion strength L_{md} can be

written in terms of local mass distortion/variation Δm and corresponding spatial correlation decay length (l_c) [20].

$$L_{md} \propto \Delta m l_c$$

Representatives of the corresponding local L_{md} images of cells and their respective average values are shown in Fig. 7B and C. The results show effective morphological distortion, L_{md}, in the samples/areas where MUC13 and HER2 co-localization was observed as compared to the adjacent areas or individual samples where no co-localization was observed (Fig. 7B and C). The results suggest that MUC13 and HER2 co-localization is associated with the increase of nano to submicron scale morphological distortion (mass-density variation), which accounted for the increasing degree of carcinogenesis [19, 20].

Discussion

HER-2 expression has been established as a potential mediator of growth factor-related signal transduction in PDAC. Therefore, it is of great interest to explore its possible regulatory relationship between various signaling moieties that might lead to its ligand induced activation and facilitate development of pancreatic malignancy. Numerous studies suggest that mucins mediate interactions between various proteins to create a favorable environment for tumor progression [21]. The altered expression pattern of MUC13 is observed in PDAC, from the early neoplastic lesion, Pancreatic Intraepithelial Neoplasia (PanIN), to invasive pancreatic carcinomas[22]. Interestingly, exogenous MUC13 was found to increase the expression of HER2, which suggests its possible correlation with the expression/activation of HER2 [2, 22]. This report provides, for the first time, experimental evidence and significance of the interaction of MUC13 and HER2 in PDAC cells.

We present evidence to support an interaction between MUC13 and HER2 in PDAC cells/tissues and a new paradigm for the biological function of the interaction. We demonstrate how MUC13 interaction with HER2 and its subsequent activation are prerequisite for the MUC13 induced cellular transformation in PDAC cells by HER2 knockdown. MUC13 co-localization/binding to HER2 in PDAC tissues and not in normal pancreatic tissues clearly indicates the potential clinical significance of this novel interaction. Although MUC13 and HER2 co-localization was observed in some tumor adjacent normal samples (4 out of 39 samples), the intensity and the percentage of co-localization was fairly less than PDAC samples. We confirmed that stable expression of MUC13 leads to increased HER2 activation and modulates the downstream signaling events which are significantly abrogated on HER2 knockdown. This study, for the first time, demonstrates a direct binding of HER2 to EGF-like domains in MUC13, EGF1 and EGF2 but not EGF3, proceeding to increased phosphorylation of HER2 and its downstream signaling which is known to regulate growth, motility or differentiation properties of the cell [23]. Additionally, our immunofluorescence results revealed that the multiplicity of MUC13 on the surface of cancer cells was accompanied by reorganization of the actin cytoskeleton. We speculate that MUC13 binds to and stabilizes HER2, activates the HER2 signaling, leading to the activation of PAK-1. This further increases the physical association between activated HER2, PAK1, and F-actin, and a

redistribution of PAK1 at the cellular projections. This is how MUC13 augments increased migration and enhanced invasion in MUC13 expressing cells. Additionally, we found that phosphorylated status of signaling components (as well as the total proteins) was significantly abrogated upon HER2 knockdown, revealing a paramount role of HER2. However, the reason that we do not see much changes in the total levels of these proteins may be either due to the transient effects of HER2 silencing or the involvement of other regulatory mechanisms that are modulated on exogenous MUC13 expression.

In order to gain further insight into the MUC13 dynamics, we investigated if MUC13 has a role in potentiation of integrin signaling. Like other bulky glycoproteins, MUC13 imparts steric hindrance and decreases the accessibility of integrins to their ligands to form adhesion complexes, thus reducing the overall integrin-binding rate[5, 24, 25]. We observed reduced adherence in MUC13 expressing cells due to difference in the size of mucins (~200–2000 nm)[26] as compared to integrins (~20 nm) [25] which was restored on MUC13 clustering at the cell surface into patches following incubation with monoclonal MUC13 antibody. However, our further experiments revealed slightly increased clustering of Integrin-α-5 and vinculin at the focal adhesions of MUC13 expressing cells as compared to MUC13 null cells. We noted that whereas MUC13 expressing cells lead to integrin clustering, it could not physically alter integrin state and cause adhesion of cells. The probable explanation to this lies in the dynamics of adhesion complexes that can be formed by establishment of increasing integrin-ligand interaction and varying glycosylation patterns of mucins [25]. Therefore, our observations implicate the role of MUC13 in potentiation of HER2 signaling and its negative effect on integrin signaling.

Next, we attempted to study the changes in the internal architecture of the cells outside of the spatial extent of tumors in PDAC samples and investigate if any association can be quantified with MUC13 and HER2 interaction. The increased nanoscale architectural changes in tumor tissues displaying MUC13 and HER2 interaction depict increased aggressiveness and malignant properties of the tumor [16, 18, 20]. These studies do not provide definitive information about the evaluation of disorder strength due to interaction of MUC13 with HER2. However, from the clinical perspective, some insight can be gleaned by our observation depicting the relevance and importance of MUC13 and HER2 signaling in PDAC. To our knowledge, this is the first study that implies the significance of physical interactions among proteins in rendering nanoscale architectural alterations in the field of carcinogenesis. Future studies are warranted to ascertain the clinical potential of this novel paradigm with respect to various stages of cancer that can help to identify patients harboring malignant disease.

Thus, herein, we provide experimental evidence for the interaction of MUC13 and HER2 in PDAC. These results elucidate a mechanistic role of MUC13 in the modulation of HER2 mediated cellular signaling in PDAC (Fig. 7D). Furthermore, our findings suggest the correlation of MUC13-HER2 interaction with increased nanoscale disorder and degree of tumorigenicity. Therefore, it further warrants future studies to establish clinical importance of the interaction to identify patients harboring aggressive PDAC tumors.

Materials and Methods

Cell culture, antibodies and procurement of PDAC tissue samples

The human PDAC cell lines purchased from ATCC were grown in recommended growth medium supplemented with 10% fetal bovine serum and antibiotics. The cells were grown at 37°C with 5% CO_2 in a humidified atmosphere. All cell lines were recently authenticated and tested for mycoplasma contamination. All cell lines were maintained in continuous exponential growth by passaging twice a week in cell type-specific media. To investigate the co-localization patterns of MUC13 and HER2 in normal pancreas, adjacent normal and PDAC samples, TMAs were obtained from John Hopkins (JHUTMA.641), University of Nebraska Medical Center (TMA#PA2012), US Biomax (OD-CT-DgPan03-001), UTHSC-Baptist TMA. The use of archived clinical samples in this study is approved by the institutional review board (IRB) at UTHSC and Baptist Memorial Hospital, Memphis.

Generation of MUC13 expressing/knockdown stable cell lines and HER2 knockdown

MUC13 null PDAC cells, MiaPaca and Panc-1, were transfected with human MUC13 cloned in pcDNA3.1 or the empty vector using XtremeGene HP (Roche) following the manufacturer's protocol. Two stable transfected clones of MiaPaca (referred to as MiaP-M13A and MiaP-M13B) and one of Panc-1 (referred to as Panc-1-M13) were selected, as previously described [2]. MUC13 knockdown HPAF-II cells were generated as described earlier to achieve stable long term MUC13 silencing [2] (shMUC13A and shMUC13B). HER2 knockdown in cells was performed using HER2 siRNA (Santa Cruz).

Construction of MUC13 deletion mutants

We constructed three MUC13 EGF-like domain deletion mutants (MUC13 ΔEGF 2/3, MUC13 ΔEGF 1/3, and MUC13 ΔEGF 1/2) each having intact EGF-like binding domains 1, 2 and 3, respectively (Fig. 4). PCR reactions were carried out using deep vent DNA polymerase as per the protocol provided (*NEB*). Xho1 and BamH1 restriction digestion sites in pEGFP-N1 were used for the ligation of the deletion mutants (Fig. S5). The transfections were performed using Lipofectamine 2000^{TM} reagent (Invitrogen) according to manufacturer's instruction.

Reciprocal Co-Immunoprecipitation

Co-Immunoprecipitation (Co-IP) was performed in MUC13 expressing HPAF-II and AsPC-1 cells. Equal amounts of protein (300 μg) were incubated with antibodies using protein A/G Sepharose beads followed by incubation at 4 °C for 4 h. Immunoprecipitates were eluted using SDS sample buffer (Santa Cruz Biotechnology) [27].

Immunoblotting

The immunoprecipitates were resolved on SDS-PAGE and immunoblotted with anti-MUC13 MAb (produced in our lab # clone PPZ020) and anti-HER2 PAb (catalog number A0485; Dako). The proteins were analyzed by immunoblotting with pHER2^{Y1248} (catalog number 2247), FAK (catalog number 3285), pFAK ^{Y925} (catalog number 3284), ERK1/2 (catalog number 9102), pERK (catalog number 9101), pAKT^{Th308} (catalog number 2965), AKT

(catalog number 9272), PAK (catalog number 2602), pPAK1 (catalog number 2605), Integrin-α4 (catalog number 8440), vinculin (catalog number 13901) α-tubulin (catalog number 2144) that were purchased from Cell Signaling [28]. The integrin-α5 (catalog number AB1928) was purchased from EMD Millipore. Mouse (catalog number 4021) and rabbit (catalog number 4011) horseradish peroxidase-conjugated secondary antibodies were purchased from Promega.

Confocal immunofluorescence and Proximity Ligation Assay

Confocal immunofluorescence was performed as described earlier [22]. Briefly, cells were fixed and incubated with mouse monoclonal anti-MUC13 antibody and/or rabbit polyclonal anti-HER2 antibody (Dako) for 1 h followed by co-localization and PLA assay. Co-localization of MUC13 and HER2 was analyzed by further incubating cells with Alexa Fluor 488 goat anti-Mouse (catalog number A11029) or Alexa Fluor 568 goat anti-Rabbit (catalog number A11036) secondary antibodies (Thermo Fisher Scientific) for 1 h [22]. In order to investigate the influence of MUC13 on the spatial distribution of integrins, we double stained Panc-1-V and Panc-1-M13 cells with integrin-α5 or vinculin with F-actin. The secondary antibodies used were Cy5 Goat anti-Rabbit (far red; pseudo color grey) for integrin-α5 and vinculin (catalog number A10523; Thermo Fisher Scientific) and phalloidin red (TRITC) staining for F-actin followed by analysis using confocal immunofluorescence.

PLA was performed using the Duolink Red Starter PLA Kit according to the manufacturer's instructions. PLA enables to simultaneously detect the subcellular localization of endogenous protein–protein interactions at single molecule resolution. Briefly, Oligonucleotide-conjugated anti-mouse minus and anti-Rabbit plus PLA secondary probes were added and incubated in a humidified chamber for 1 h at 37 °C. Oligonucleotides were hybridized and circularized by ligation for 30 min at 37 °C followed by incubation with DNA polymerase for 100 min at 37 °C to produce rolling circle amplification products tagged with a red fluorescence probe. The nuclei were counterstained with DAPI and visualized using a Nikon Confocal microscope.

Co-capping Assay

MUC13 expressing HPAF-II, AsPC-1 and Panc-1 cells were incubated with Tetramethylrhodamine (TRITC) labeled anti-MUC13 MAb (25 μg/ml) for 1 h at 4 °C and plated for 2 h at 37 °C for adherence. Cells were fixed and permeabilized with Triton X-100. Cells were then incubated with anti-HER2 antibody (Dako) or α-tubulin (negative control) for 1 h followed by incubation with FITC goat anti-Rabbit secondary antibody (catalog number 65-6111; Thermo Fisher Scientific) followed by confocal microscopy [22].

Cell Adhesion Assays

Panc-1-V and Panc-1-M13 cells (0.5×10^4/24 well) were seeded onto collagen, fibronectin, and poly-L-lysine-coated plates for 1 h at 37°C. The cells that adhered to the wells were counted using automated cell counter (Cell Countess, Invitrogen). Additionally, cells (4×10^3/24 well) were seeded on anti-integrin-α4 or α5 antibody coated plates for 1 h followed by addition of 20 μL of MTS reagent to each well at 37 °C for 2.5 h and measured for absorbance. To further confirm the role of MUC13 in the inhibition of integrin mediation

adhesion, cells were preincubated with Alexa-Fluor 647-labelled MUC13 monoclonal antibody and then allowed to adhere on the integrin coated plates.

Cell Proliferation, Motility, Invasion and Anchorage-dependent Colony Forming Assay

MUC13 null Panc-1 cells were transfected with MUC13 EGF-like domain deletion mutant constructs (MUC13 ΔEGF 2/3, MUC13 ΔEGF 1/3 and MUC13 ΔEGF 1/2). Cell proliferation and invasion assays were performed by using MTS reagent and Matrigel invasion chambers (BD Biosciences) respectively, as described earlier [22]. Changes in cell motility were determined through wound healing/scratch [22] and agarose bead-based cell motility assays as described earlier [2, 29] using HPAF-II, Panc-1-V (vector control), and Panc-1-M13 (MUC13 over-expressing) cells. For the anchorage-dependent colony-forming assay, cells (5×10^3/100 mm dishes) were incubated for 10 days and stained with hematoxylin [2].

Confocal double immunofluorescence analysis of PDAC tissues for MUC13 and HER2

Immunohistofluorescence analysis of formalin-fixed paraffin-embedded human pancreatic tumor tissues was performed by deparaffinizing and rehydrating the tissues followed by antigen retrieval. The tissue sections were blocked with 10% donkey serum and labelled with the primary antibodies against HER2 (anti-rabbit) in 5% donkey serum (the species in which the secondary antibodies are raised) overnight. Next day, tissues were labelled with Alexa Fluor® 488 conjugated (green) secondary antibody [donkey anti-Rabbit IgG (H+L); catalog number 711-546-152, Jackson ImmunoResearch Laboratories, Inc.] for 1 hr followed by washing in PBS and labelling with another primary antibody, anti-MUC13 MAb, overnight. After incubation, CY3 (red) conjugated secondary antibody [donkey anti-Mouse IgG (H+L); Catalog number: 715-166-151, Jackson ImmunoResearch Laboratories, Inc.] was labelled for 1 hr followed by washing thrice in PBS. The slides were mounted with VECTASHIELD Antifade Mounting Medium with DAPI and analyzed using Ziess 710 confocal microscope for MUC13 and HER2 expression and their co-localization (yellow).

Statistical analysis

Statistical analysis was presented as mean ± S.E. of at least 3 independent experiments. *P-values* <0.05 were considered statistically significant. The analysis of adjacent and cancer samples from human pancreatic ductal adenocarcinoma was done using chi-square test to compare group proportions.

Potential conflicts of interest

The authors declare that there are no financial and non-financial competing interests.

Supplementary Material

Refer to Web version on PubMed Central for supplementary material.

Acknowledgments

Financial support: Subhash C. Chauhan: This work was partially supported by grants from the Department of Defense (PC130870); the National Institutes of Health (RO1 CA142736 and UO1 CA162106A) and financial support from the Kosten Foundation for pancreatic cancer research (UT 14-0558).

Meena Jaggi: Department of Defense (PC130870); the National Institutes of Health (UO1 CA162106A) and the College of Pharmacy Dean's Seed Grant of the University of Tennessee Health Science Center.

This work was partially supported by grants from the Department of Defense (PC130870 to SCC and MJ), the National Institutes of Health (R01 CA142736 to SCC, U01 CA162106A to SCC and MJ; R01 EB003682 to PP; K22CA174841 to MMY), the College of Pharmacy 2014 and 2015 Dean's Seed/Instrument Grants of the University of Tennessee Health Science Center (to SCC, MJ and MMY) and Grants of the University of Memphis (to PP). Authors acknowledge the Herb Kosten Foundation for pancreatic cancer research support. The authors are also thankful to Cathy Christopherson for editorial assistance.

References

1. Kar G, Gursoy A, Keskin O. Human cancer protein-protein interaction network: a structural perspective. PLoS Comput Biol. 2009; 5:e1000601. [PubMed: 20011507]
2. Chauhan SC, Ebeling MC, Maher DM, Koch MD, Watanabe A, Aburatani H, et al. MUC13 mucin augments pancreatic tumorigenesis. Mol Cancer Ther. 2012; 11:24–33. [PubMed: 22027689]
3. Maher DM, Gupta BK, Nagata S, Jaggi M, Chauhan SC. Mucin 13: structure, function, and potential roles in cancer pathogenesis. Mol Cancer Res. 2011; 9:531–537. [PubMed: 21450906]
4. Settleman J. Predicting response to HER2 kinase inhibition. Oncotarget. 2015; 6:588–589. [PubMed: 25655645]
5. Chaturvedi P, Singh AP, Chakraborty S, Chauhan SC, Bafna S, Meza JL, et al. MUC4 mucin interacts with and stabilizes the HER2 oncoprotein in human pancreatic cancer cells. Cancer Res. 2008; 68:2065–2070. [PubMed: 18381409]
6. Senapati S, Das S, Batra SK. Mucin-interacting proteins: from function to therapeutics. Trends Biochem Sci. 2010; 35:236–245. [PubMed: 19913432]
7. Koos B, Cane G, Grannas K, Lof L, Arngarden L, Heldin J, et al. Proximity-dependent initiation of hybridization chain reaction. Nat Commun. 2015; 6
8. Holbro T, Hynes NE. ErbB receptors: directing key signaling networks throughout life. Annu Rev Pharmacol Toxicol. 2004; 44:195–217. [PubMed: 14744244]
9. Schaller MD. Biochemical signals and biological responses elicited by the focal adhesion kinase. Biochim Biophys Acta. 2001; 1540:1–21. [PubMed: 11476890]
10. Schlaepfer DD, Hunter T. Focal adhesion kinase overexpression enhances ras-dependent integrin signaling to ERK2/mitogen-activated protein kinase through interactions with and activation of c-Src. J Biol Chem. 1997; 272:13189–13195. [PubMed: 9148935]
11. Lauffenburger DA, Horwitz AF. Cell migration: a physically integrated molecular process. Cell. 1996; 84:359–369. [PubMed: 8608589]
12. Adam L, Vadlamudi R, Kondapaka SB, Chernoff J, Mendelsohn J, Kumar R. Heregulin regulates cytoskeletal reorganization and cell migration through the p21-activated kinase-1 via phosphatidylinositol-3 kinase. J Biol Chem. 1998; 273:28238–28246. [PubMed: 9774445]
13. Grothey A, Hashizume R, Ji H, Tubb BE, Patrick CW Jr, Yu D, et al. C-erbB-2/ HER-2 upregulates fascin, an actin-bundling protein associated with cell motility, in human breast cancer cell lines. Oncogene. 2000; 19:4864–4875. [PubMed: 11039904]
14. Parry S, Silverman HS, McDermott K, Willis A, Hollingsworth MA, Harris A. Identification of MUC1 proteolytic cleavage sites in vivo. Biochem Biophys Res Commun. 2001; 283:715–720. [PubMed: 11341784]
15. Williams SJ, Wreschner DH, Tran M, Eyre HJ, Sutherland GR, McGuckin MA. Muc13, a novel human cell surface mucin expressed by epithelial and hemopoietic cells. J Biol Chem. 2001; 276:18327–18336. [PubMed: 11278439]

16. Damania D, Subramanian H, Tiwari AK, Stypula Y, Kunte D, Pradhan P, et al. Role of Cytoskeleton in Controlling the Disorder Strength of Cellular Nanoscale Architecture. Biophysical Journal. 2010; 99:989–996. [PubMed: 20682278]
17. Pradhan P, Damania D, Joshi HM, Turzhitsky V, Subramanian H, Roy HK, et al. Quantification of nanoscale density fluctuations using electron microscopy: Light-localization properties of biological cells. Applied Physics Letters. 2010; 97:243704. [PubMed: 21221251]
18. Pradhan P, Damania D, Joshi HM, Turzhitsky V, Subramanian H, Roy HK, et al. Quantification of nanoscale density fluctuations by electron microscopy: probing cellular alterations in early carcinogenesis. Phys Biol. 2011; 8:026012. [PubMed: 21441647]
19. Subramanian H, Pradhan P, Liu Y, Capoglu IR, Li X, Rogers JD, et al. Optical methodology for detecting histologically unapparent nanoscale consequences of genetic alterations in biological cells. Proceedings of the National Academy of Sciences of the United States of America. 2008; 105:20118–20123. [PubMed: 19073935]
20. Subramanian H, Roy HK, Pradhan P, Goldberg MJ, Muldoon J, Brand RE, et al. Nanoscale Cellular Changes in Field Carcinogenesis Detected by Partial Wave Spectroscopy. Cancer research. 2009; 69:5357–5363. [PubMed: 19549915]
21. Kaur S, Kumar S, Momi N, Sasson AR, Batra SK. Mucins in pancreatic cancer and its microenvironment. Nat Rev Gastroenterol Hepatol. 2013; 10:607–620. [PubMed: 23856888]
22. Khan S, Ebeling MC, Zaman MS, Sikander M, Yallapu MM, Chauhan N, et al. MicroRNA-145 targets MUC13 and suppresses growth and invasion of pancreatic cancer. Oncotarget. 2014; 5:7599–7609. [PubMed: 25277192]
23. Jonckheere N, Van Seuningen I. The membrane-bound mucins: how large O-glycoproteins play key roles in epithelial cancers and hold promise as biological tools for gene-based and immunotherapies. Crit Rev Oncog. 2008; 14:177–196. [PubMed: 19409062]
24. Guddo F, Giatromanolaki A, Koukourakis MI, Reina C, Vignola AM, Chlouverakis G, et al. MUC1 (episialin) expression in non-small cell lung cancer is independent of EGFR and c-erbB-2 expression and correlates with poor survival in node positive patients. Journal of Clinical Pathology. 1998; 51:667–671. [PubMed: 9930070]
25. Paszek MJ, DuFort CC, Rossier O, Bainer R, Mouw JK, Godula K, et al. The cancer glycocalyx mechanically primes integrin-mediated growth and survival. Nature. 2014; 511:319–325. [PubMed: 25030168]
26. Maher DM, Gupta BK, Nagata S, Jaggi M, Chauhan SC. Mucin 13: Structure, Function, and Potential Roles in Cancer Pathogenesis. Molecular Cancer Research. 2011; 9:531–537. [PubMed: 21450906]
27. Jaggi M, Rao PS, Smith DJ, Wheelock MJ, Johnson KR, Hemstreet GP, et al. E-cadherin phosphorylation by protein kinase D1/protein kinase C{mu} is associated with altered cellular aggregation and motility in prostate cancer. Cancer Res. 2005; 65:483–492. [PubMed: 15695390]
28. Khan S, Kaur R, Shah BA, Malik F, Kumar A, Bhushan S, et al. A Novel cyano derivative of 11-Keto-beta-Boswellic acid causes apoptotic death by disrupting PI3K/AKT/Hsp-90 cascade, mitochondrial integrity, and other cell survival signaling events in HL-60 cells. Mol Carcinog. 2012; 51:679–695. [PubMed: 21751262]
29. Chauhan SC, Vannatta K, Ebeling MC, Vinayek N, Watanabe A, Pandey KK, et al. Expression and functions of transmembrane mucin MUC13 in ovarian cancer. Cancer Res. 2009; 69:765–774. [PubMed: 19176398]

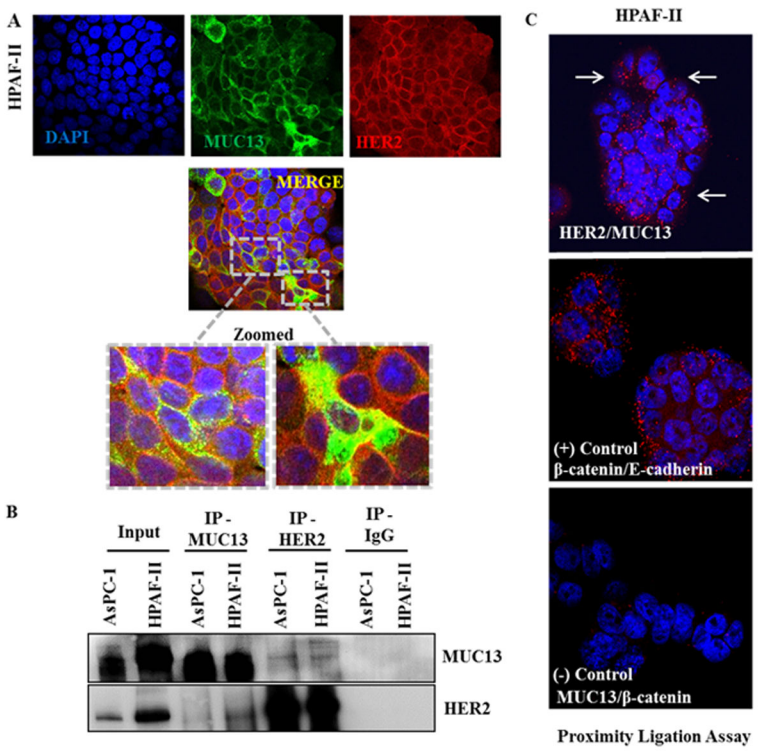

Figure 1. MUC13 and HER2 interact in PDAC cells

(A) Confocal immunofluorescence of HPAF-II cells. Cells were grown at low density on 4-well chambered coverglass slide, washed, fixed with 2% paraformaldehyde, and permeabilized before incubation with anti-MUC13 (MAb) and HER2 (PAb). This was followed by sequential acquisition of fluorescence signals. MUC13 (green) was detected by using Alexa Fluor 488 conjugated secondary antibody while HER2 was identified with Alexa Fluor 568 conjugated secondary antibody (red). Merge of MUC13 and HER2 showed co-localization (yellow). (B) Co-immunoprecipitation (co-IP) assay. Protein lysates from HPAF-II and AsPC-1 cells (endogenously expressing MUC13) were used for immunoprecipitation using mouse anti-MUC13 (MAb) and rabbit anti-HER2 (PAb) antibodies, separately. The immunoprecipitates were electrophoretically resolved on a 4–15% gradient SDS-PAGE gel and immunoblotted with anti-MUC13 or anti-HER2 antibodies. The respective nonspecific IgG (mouse or rabbit IgGs) was used for IP controls. (C) *In situ* proximity ligation assay (PLA). PLA on HPAF-II cells was performed using the Duolink Red Starter PLA Kit. The nuclei were counterstained with DAPI, and visualized using a Nikon Confocal microscope. Red spots indicate HER2/MUC13 interactions. In this experiment, β-catenin and E-cadherin were used as positive (+) control while MUC13 and β-catenin served as negative (−) control. Data are the representation of three independent experiments. Pictures original magnification, A 200X; C 400X.

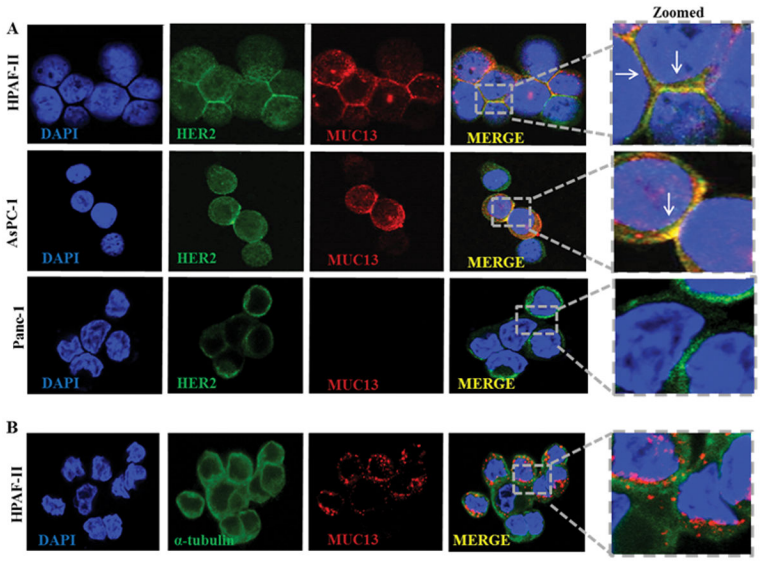

Figure 2. MUC13 and HER2 exist in a complex in pancreatic cancer cells

(A) HPAF-II, AsPC-1 and Panc-1 cells in suspension were incubated with TRITC and Alexa-Fluor 647 (in the case of Panc-1) -conjugated MUC13 antibody for 1 h at 4 °C. After washing, cells were seeded on 4-well chamber slides and incubated for 2 h at 37 °C for adherence. Cells were then fixed, washed, and incubated with anti-HER2 rabbit polyclonal antibodies for 60 min. After washing, cells were incubated with FITC-conjugated anti-Rabbit secondary antibody for 60 min. Immunofluorescence was detected by a confocal microscope (original magnification, 600X). The digital merging shows that HER2 co-localizes with MUC13 at the membrane in HPAF-II and AsPC-1 cells, while this co-localization is not evident in MUC13 null Panc-1 cells. (B) HPAF-II cells in suspension were incubated with Alexa Fluor-647 conjugated MUC13 antibody for 1h followed by seeding of cells and incubation with anti-α-tubulin that served as a negative control in this experiment. Images are the representation of three independent experiments.

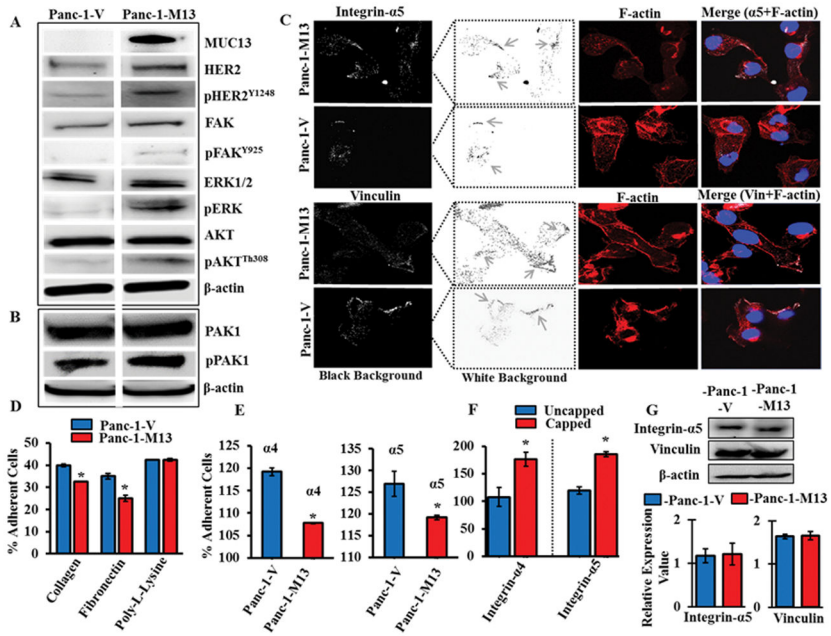

Figure 3. MUC13 interaction regulates HER2 and its downstream signaling events

(A and B) Immunoblotting of whole cell lysates. The cell lysates were prepared from stably MUC13 expressing cells (Panc-1-M13) and vector controls (Panc-1-V). The lysates were run on 4–15% gradient SDS-PAGE and immunoblotted with specific indicated antibodies. β-actin served as an internal control. The data are representative of three independent experiments. (C) Confocal immunofluorescence. Panc-1-V and Panc-1-M13 cells were seeded on collagen coated plates (rat tail collagen-1) overnight and then double stained with integrin-α5 or vinculin with F-actin. The secondary antibodies used were CY5 (far red; pseudo color grey) for integrin-α5 and vinculin and phalloidin red (TRITC) for F-actin. Original Magnification 400X. (D) Cell adhesion assay. Panc-1-V and Panc-1-M13 cells were allowed to adhere on collagen-1 or fibronectin or poly-L-Lysine coated plates for 1 h followed by counting adhered cells using cell countess. (E) Integrin mediated cell adhesion assay. Panc-1-V and Panc-1-M13 were seeded on anti-integrin-α4 and α5 coated plates for 1h followed by addition of 20 μL of MTS dye to each well at 37°C for 2.5 h and measurement of absorbance. (F) The cells were pre-incubated with Alexa-Fluor 647-labeled MUC13 monoclonal antibody and then allowed to adhere on the integrin coated plates. Bars represent mean; SEM, n=3. *indicates $p<0.05$. (G) Immunoblotting analysis of integrin-α5 and vinculin in Panc-1 and Panc-1-M13 cells. Densitometry analysis to determine the fold differences in protein expression. Intensities of immunoreactive bands on Western blots shown in Figure 3G were quantified by densitometry analysis using Gel Quant software. Data are the representation of three replicates.

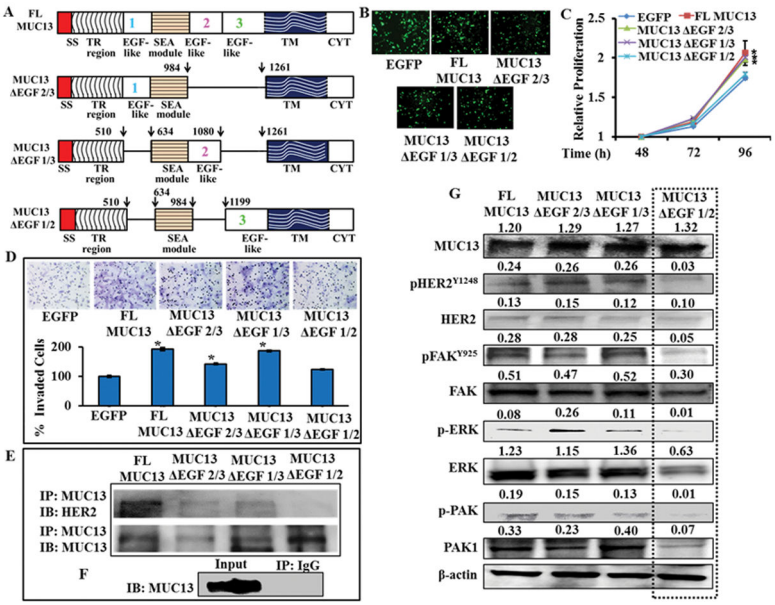

Figure 4. MUC13 domain specific interaction analysis with HER2

(A) Schematic representation of the construction of MUC13 mutants with deletions in the EGF-like domains. Briefly, the first deletion mutant of the MUC13 (MUC13 ΔEGF 2/3) was constructed by excision of EGF 2 and 3. The resultant MUC13 plasmid contains only EGF 1. The next deletion mutant (designated MUC13 ΔEGF 1/3) contains EGF 2 and was constructed by deletion of EGF 1 and 3. The third deletion mutant (MUC13 ΔEGF 1/2) contains EGF 3 and was constructed by excision of EGF 1 and 2. (B) Representative images of Panc-1 cells showing GFP fluorescence when transiently transfected with MUC13 deletion mutant constructs. (C) Proliferation assay. Changes in the proliferation of cells when transfected with different deletion mutants. Effect on cell growth was monitored by MTS assay which is shown as percentage. (D) Invasion assay. Images depicting the effect of different deletion mutants on the invasion of Panc-1 cells. Cells were photographed and counted using an imaging system. The bar graphs represent the average number of cells invaded in each case. Bars represent mean ± SEM; n=3; *p<0.05. (E) Immunoprecipitation (IP) Assay. Panc-1 cells, after transfection with MUC13 deletion mutant constructs, were immunoprecipitated with MUC13 and immunoblotted with HER2. (F) MUC13 expressing HPAF-II cells were used as input and IgG was used as a negative (−) control for this IP assay. (G) Immunoblotting experiment depicting the effect of MUC13 EGF deletion mutations on HER2 and its downstream effectors. Intensities of immunoreactive bands on Western blots shown in Figure 4G were quantified by densitometry analysis using Gel Quant software.

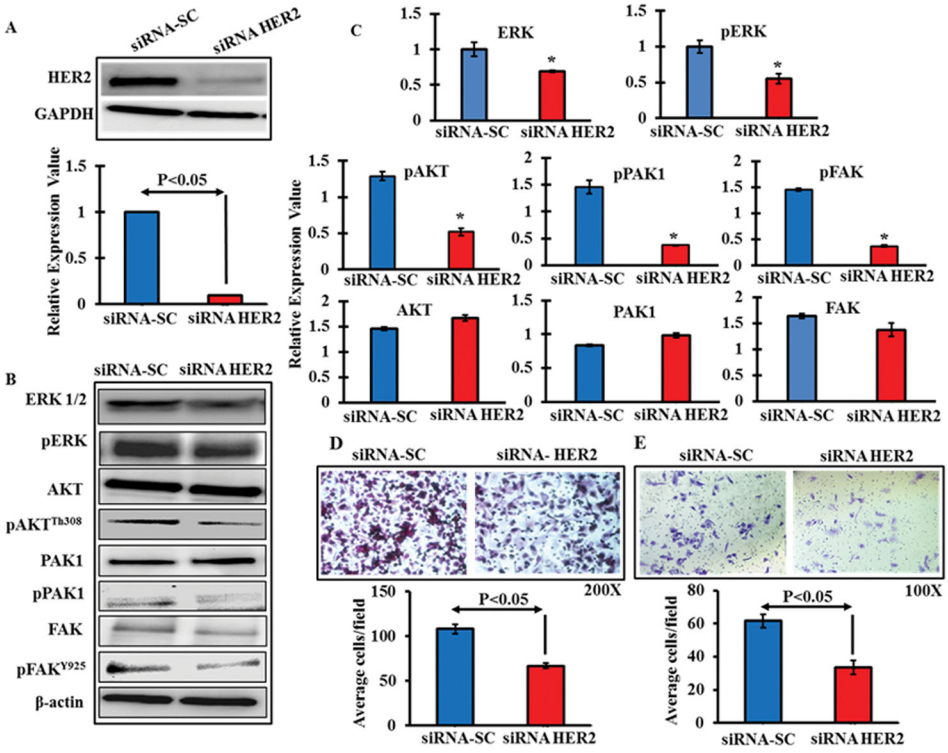

Figure 5. HER2 knockdown abrogates MUC13 cellular transformation

(A and B) Panc-1-M13 cells (0.5×10^6) were transfected with HER2 siRNA using lipofectamine 3000. Cell lysates were prepared for immunoblotting using indicated specific antibodies. (C) The corresponding bar graphs represent the densitometry analysis of protein expression that was quantified using Gel Quant software. (D) Boyden chamber migration assay. The HER2 knockdown cells were seeded on Boyden chambers for 24 h and analyzed for the effect of HER2 knockdown on cell migration. (E) Matrigel invasion assay. The HER2 knockdown cells were seeded on BD Matrigel invasion chambers for 48 h and analyzed for the effect of HER2 knockdown on cell invasion. The corresponding bar graphs are plotted against average cells/field. Bars represent mean ± SEM; n=3; *p<0.05.

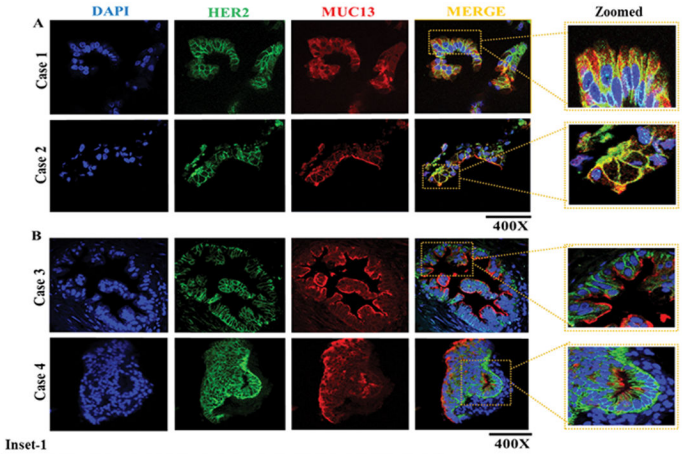

Inset-1

Cases	Total Samples	% Positive samples			*P* Value (Tumor vs Adjacent Normal)
		MUC13, *n* (%)	HER2, *n* (%)	Colocalize, *n* (%)	
Tumor	131	110 (83.9)	75 (57.2)	50 (38.1)	0.001
Adjacent Normal	39	20 (51.2)	7 (17.9)	4 (10.2)	-
Normal	3	1 (33.3)	1 (33.3)	0	-

Inset-2

Cases	% Samples showing Co-localization, *n* (%)			
	5-25	26-50	51-75	76-100
Tumor	26 (52)	18 (36)	3 (6)	3 (6)
Adjacent normal	2 (50)	2 (50)	0	0

Figure 6. Analysis of adjacent and cancer samples from human pancreatic ductal adenocarcinoma for MUC13 and HER2 co-localization

Representative images showing MUC13 and HER2 co-localization patterns in human PDAC tissues. Representative images of the pancreatic adenocarcinoma patient samples exhibiting MUC13 and HER2 co-localization. Digital merging of the immunostained tissue section depict strong co-localization (yellow) patterns of MUC13 (red) and HER2 (green) in pancreatic ductal adenocarcinoma lesions (A) and samples showing distinct staining patterns of MUC13 and HER2 and no co-localization (B). Original magnification, 400X. Corresponding Inset 1: Immunohistochemical analysis of MUC13 and HER2 to determine their co-localization in normal and PDAC samples. Inset 2: Percentage of tissue showing MUC13 and HER2 co-localization.

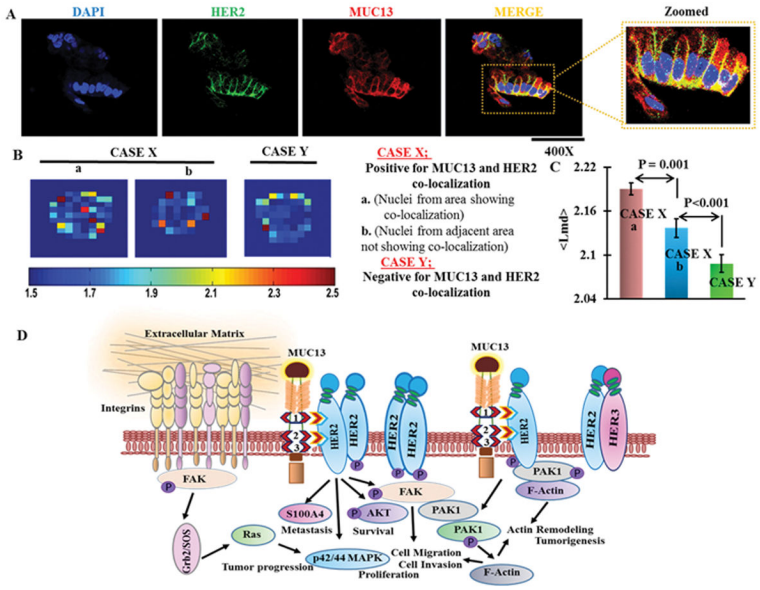

Figure 7. MUC13 and HER2 co-localization correlates with nanoscale morphological/ architectural changes in human PDAC tissues

(A) Immunohistofluorescence analysis was performed on the tissue sections to study the interaction between MUC13 and HER2. Digital merging of the immunostained tissue section depict strong co-localization (yellow) patterns of MUC13 (red) and HER2 (green) in pancreatic ductal adenocarcinoma lesions. Original magnification, 400X. (B) Representative local L_{md} distribution in two dimension images derived from the corresponding confocal image slices of nuclei for different cases; CASE X: area positive (a) and negative (b) for MUC13 and HER2 co-localization, and Case Y: negative for MUC13 and HER2 co-localization. (C) Bar plots of effective average morphological distortion, L_{md}, for the different cases (6 cases averaged over 30 cells for each case). Plots show that the morphological distortion increases in the areas displaying MUC13 and HER2 co-localization within the tissue sample from each case as compared to the adjacent areas and/or individual case, not displaying the co-localization. (D) Schematic representation of the role of MUC13 and HER2 interaction in pancreatic carcinogenesis.